Characterization of non-stationary sources using three imaging techniques

M.-H. Moulet[a], M. Melon[b], J.-H. Thomas[a] and E. Bavu[b]

[a]Laboratoire d'acoustique de l'université du Maine, Bât. IAM - UFR Sciences Avenue Olivier Messiaen 72085 LE MANS CEDEX 9
[b]Conservatoire National des Arts et Métiers, 292 rue Saint-Martin 75141 Paris Cedex 03
marie-helene.moulet@univ-lemans.fr

Over the last decades, different imaging techniques have been developed to characterize and localize non-stationary acoustic sources. This study focuses on three of them: Time Domain Holography (TDH), Sonic Time-Reversal Sink imaging (TRS) and Real-Time Near-field Acoustic Holography (RT-NAH). In the present study, we first briefly recall the principles of these methods and detail the validation technique used to compare the reconstruction quality of the three proposed imaging techniques. In the second part of this paper, a comparison is drawn between results assessed using TDH, TRS, and RT-NAH for point-like sources in a semi-anechoic room. Advantages and drawbacks of each method are discussed. The reconstruction quality is studied as a function of distance between source plane and microphone array. We also detail the influence of the frequency content radiated on reconstruction quality.

1 Introduction

The inverse problem of identification, localization and characterization of acoustic sources have received attention from the scientific community over the last decades. Different imaging technique categories have been proposed in order to solve this problem from pressure measurements on a microphone array nearby the source plane, such as acoustic holography or sonic time reversal imaging. Some recent developments of these techniques led to localize and characterize precisely both in time and space domains non-stationary or transient acoustic sources. The present paper aims at comparing three of them: Time Domain Holography (TDH), Sonic Time-Reversal Sink imaging (TRS) and Real-Time Nearfield Acoustic Holography (RT-NAH). These methods are experimentally applied to the case of point-like sources in a semi anechoic room (baffled 5 cm diameter Aurasound® NSW2-326-8A) driven by transient signals. In this paper, we first recall the principles of the three methods and the experimental set-up. Different reconstruction quality indicators in space and time domains are also introduced. Using these indicators, we study the ability of the three methods to back-propagate efficiently and precisely the pressure field. We also detail the influence of back-propagation distance on reconstruction quality. The influence of transient signals frequency content is also investigated for two back-propagation distances.

2 Theoretical background

Table 1: Schematic diagram of the three imaging methods

$P(k_x, k_y, z_m, t)$	$\Rightarrow$ **RT-NAH** $\Rightarrow$	$P(k_x, k_y, z_{ref}, t)$
$\uparrow$ $TF_{x,y}$		$\downarrow$ $TF^{-1}_{x,y}$
$p(x, y, z_m, t)$	$\Rightarrow$ **TRS** $\Rightarrow$	$p(x, y, z_{ref}, t)$
$\downarrow$ TF_t		$\uparrow$ TF^{-1}_t
$P(x, y, z_m, \omega)$		$P(x, y, z_{ref}, \omega)$
$\downarrow$ $TF_{x,y}$		$\uparrow$ $TF^{-1}_{x,y}$
$P(k_x, k_y, z_m, \omega)$	$\Rightarrow$ **TDH** $\Rightarrow$	$P(k_x, k_y, z_{ref}, \omega)$

Table 1 synthetically presents the imaging methods used in this study to backward propagate time-dependent pressure fields. These methods involve pressure measurements $p(x, y, z_m, t)$ on a microphone array at a distance z_m from the source plane. $p(x, y, z_{ref}, t)$ corresponds to the back-propagated (BP) time-dependent pressure signal at a distance z_{ref} from the source plane; $P(k_x, k_y, z_i, t)$ is the time-dependent wavenumber spectrum at z_i; $P(x, y, z_i, \omega)$ is the frequency spectrum at z_i and $P(k_x, k_y, z_i, \omega)$ is the frequency-wavenumber spectrum at z_i.

2.1 Time Domain Holography (TDH)

Time Domain Holography makes use of time and 2D-space Fourier transforms of the measured pressure field $p(x, y, z_m, t)$ to compute the pressure spectrum $P(k_x, k_y, z_m, \omega)$. Then, the backward propagation is processed by using classical NAH for each angular frequency. Finally, inverse time and 2D-space Fourier transforms are applied to the backward propagated spectrum in order to recover the time-space signals $p(x, y, z_{ref}, t)$. As this problem is ill-posed, regularization techniques have to be used in order to obtain a reliable solution. In this paper, the Tikhonov filter in its standard form is applied. Since the reference field is measured in the experiments conducted here, the optimal filter parameter was chosen as the one which gave the lowest differences between the reference and the backward propagated fields. Mathematical details of this method could be found in refs. [1, 2].

2.2 Real-Time Nearfield Acoustic Holography (RT-NAH)

Real-Time Near-field Acoustic Holography is based on a formulation which describes the propagation of time-dependent sound pressure signals on a forward plane (direct problem) using a convolution product between the measured sound field and an impulse response in the time-wavenumber domain [3]. Thus, this method does not involve calculations in the frequency domain. In order to obtain the sound field on the source plane, it is necessary to solve an inverse problem using deconvolution. The time-dependent wavenumber spectrum on the source plane is obtained from the convolution between the time-dependent wavenumber spectrum acquired by the microphone array and an inverse impulse response. This inverse impulse response - which depends on the distance between the source plane and the measurement plane and also on the wavenumber considered - can be computed by at least two methods. The first one, which was used in this study, is based on inverse Wiener filtering of the direct impulse response [4]. The second one uses a Singular Value Decomposition to invert a matrix describing the direct propagation in the time-wavenumber domain, coupled to a standard Tikhonov regularization [5]. Both approaches yield a continuous time reconstruction of the pressure field on the source plane.

2.3 Sonic Time-Reversal Sink imaging (TRS)

Sonic time reversal sink (TRS) imaging technique is computed in the space-time domain and does not involve any Fourier transform. Classical time-reversal (TR) procedures ensure that if a pressure field $p(\vec{r}, t)$ is solution of the wave equation, the time-reversed acoustic field $p(\vec{r}, -t)$ has a math-

ematical and physical existence [6]. Using a time-reversed version of the time domain Helmholtz-Kirchhoff equation (HK), a focusing pressure field $p_{TR}(\vec{r},t)$ can be BP in (V) using measurements of the acoustic pressure and its normal derivative on a surface (S) surrounding the volume (V). $p_{TR}(\vec{r},t)$ has the property to back-propagate to the acoustic sources positions and to reconstruct the time evolution of the radiated field at focal point, thus allowing to partially solve the inverse problem and to localize and image acoustic radiating sources. However, $p_{TR}(\vec{r},t)$ using *classical* TR imaging is not strictly equal to $p(\vec{r},-t)$, since the TR back-propagation gives rise to a divergent wave following the convergent focusing wave [7, 8]. In order to completely solve the inverse problem and to assess the exact dual pressure field $p(\vec{r},-t)$, TRS imaging method has been proposed [8], using a numerical sink source located at focal point, that emits the exact pressure field that destructively interferes with the unwanted diverging component of $p_{TR}(\vec{r},t)$. When a single layer measurement array is used as it is in this study, TRS technique has also the advantage of giving access to an approximation of the normal derivative of measured pressure field involved in HK equation, thus improving field reconstruction. Detailed physical and mathematical explanations of this method in the sonic range and its implementation can be found in [8].

3 Material and Methods

3.1 Experimental set-up

A 10×10 microphone array is used to simultaneously measure the radiated acoustic pressure (Figure 1) at a sampling frequency of 32768 Hz. Adjacent microphones are regularly spaced by 8.5 cm, corresponding to an array size of 76.5×76.5 cm. This experimental set-up ensures frequencies included in the $[440 - 2000]$ Hz range respect the space domain Shannon theorem. Measurements are achieved at a distance from source plane varying from 5 cm to 25 cm by 5 cm steps. Reference pressure p_{ref} is measured by the array at $z_{ref} = 1$ cm, thus allowing to calculate objective indicators in order to assess the relevance and precision of the methods.

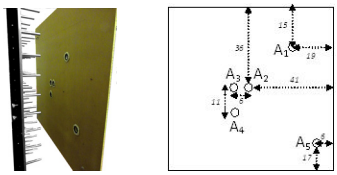

(a) (b)

Figure 1: Microphone array in front of sources (a) and repartition of loudspeakers in the source plane (b).

Five small baffled loudspeakers (5 cm diameter Aurasound® NSW2-326-8A) are fixed on a plane of larger dimensions than the array. Positions of the loudspeakers are given for reference in Figure 1. Each loudspeaker is sequentially driven by a transient signal. Six different central frequencies f_c are used for the broadband impulse signals (Hanning-window spectra from 0 Hz to 2 f_c) : $f_c \in [425, 750, 1000, 1335, 1865, 2000]$ Hz. The aim of this study is to reconstruct the sound field on the plane $z_{ref} = 1$ cm from the sound field measured by the microphone array on the plane z_m.

3.2 Reconstruction quality indicators

In order to compare the results obtained with the three methods, two reconstruction quality indicator maps (T_1 and T_2) are calculated for a point (x_i, y_j) of the source plane. They are similar to those used in [5]. T_1 is a correlation coefficient which is sensitive to the similarity between the shapes of the signals and thus between their phase difference. The best value for T_1 is 1. T_2 is sensitive to the magnitude differences between the reconstructed signals and the references. The best value for T_2 is 0. The following equations (1) and (2) define T_1 and T_2 :

$$T_1(x_i,y_j) = \frac{< p_{ref}(x_i,y_j,z_{ref},t)p(x_i,y_j,z_{ref},t) >_t}{p_{ref}^{rms}(x_i,y_j,z_{ref})p^{rms}(x_i,y_j,z_{ref})}, \quad (1)$$

$$T_2(x_i,y_j) = \frac{|p_{ref}^{rms}(x_i,y_j,z_{ref}) - p^{rms}(x_i,y_j,z_{ref})|}{p_{ref}^{rms}(x_i,y_j,z_{ref})}, \quad (2)$$

where $p_{ref}(x_i,y_j,z_{ref},t)$ is the reference time dependent pressure signal and $p(x_i,y_j,z_{ref},t)$ is the BP time-dependent pressure signal. In Eq.(1), $<>_t$ is the time averaged value. In order to evaluate the quality of back-propagation as a function of time, a third criterion is defined (Eq. (3)), which describes a mean spatial error of reconstruction. Perfect reconstructions yield $E_n(t) = 0$.

$$E_n(t) = \frac{\sqrt{< [p_{ref}(x,y,z_{ref},t) - p(x,y,z_{ref},t)]^2 >_s}}{< p_{ref}^{rms}(x,y,z_{ref}) >_s}, \quad (3)$$

where $<>_s$ is the spatial averaged value.

4 Results and discussion

4.1 Time domain back-propagation

An example of back-propagated (BP) pressure at a single position corresponding to microphone $(4,4)$ is presented on Figure 2 and compared with the measured reference pressure at the same position. The position of microphone (4,4) is indicated for reference on figure 3. In Figure 2, TDH method seems to give the closest results in terms of amplitude, when compared to the reference pressure. T_2 values for this microphone confirm this statement : $T_2^{TDH}(4,4) = 0,04$, $T_2^{RT-NAH}(4,4) = 0,08$ and $T_2^{TRS}(4,4) = 0,08$.

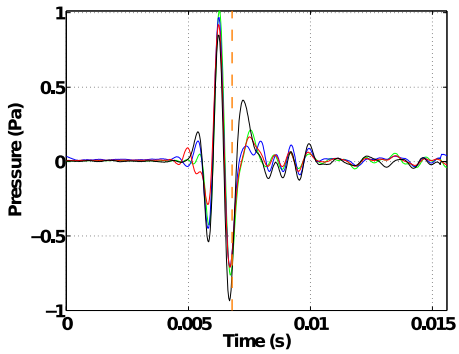

Figure 2: Comparison of BP pressures from $z_m = 10$ cm to z_{ref} with the measured reference pressure on microphone $(4,4)$ position when loudspeaker A_2 emits a 1000 Hz impulse. Green: reference pressure - Blue: TDH - Red: TRS - Black: RT-NAH - Orange vertical dotted line indicates $t_s = 6.77$ ms

In terms of phase reconstruction, TRS results present a slight phase difference before the impulse signal ($T_1^{TRS}(4,4) = 0,90$) while for the two other methods,

results present a slight phase difference at the end of the impulse signal ($T_1^{TDH}(4,4) = 0,96$ and $T_1^{RT-NAH}(4,4) = 0,88$).

A comparison of BP pressure fields at a single time (t_s = 6.77 ms, indicated for reference in Fig. 2) with the reference pressure field measured at 1 cm is also given in Figure 3 for a 1000 Hz signal on source A_2. This figure shows that for the time considered, there is a good agreement with the reference field for TDH methods ($E_n^{TDH}(t_s) = 0,86$). TRS results show at this particular time a slightly underestimated pressure level ($(E_n^{TRS}(t_s) = 1,56$). RT-NAH results show at this particular time some spatial distortions and the level at source location is not estimated accurately ($E_n^{RT-NAH}(t_s) = 1,96$).

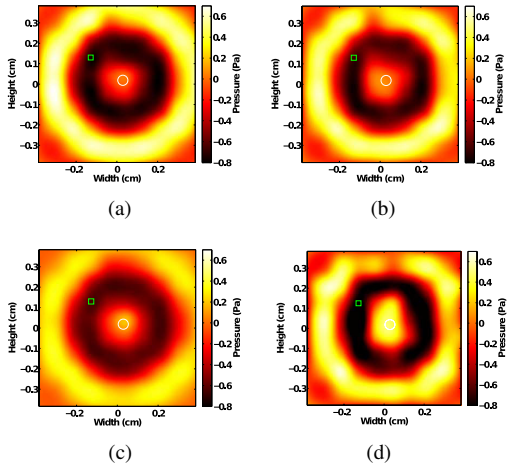

Figure 3: BP pressure fields maps at t = 6.77 ms: reference measured at 1cm (a), obtained with TDH (b), TRS (c), and RT-NAH (d). Case of a 1000 Hz impulse BP from 10 cm to 1 cm for A_2. The white circle represents the source position and size. The green square on (a) represent the position of microphone (4,4).

4.2 Reconstruction quality indicators

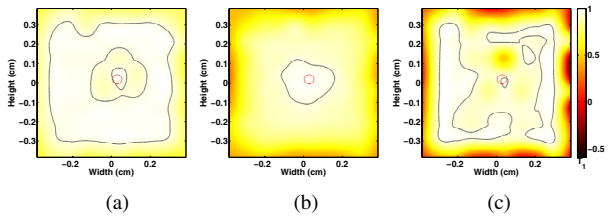

Figure 4: Spatial maps for indicator T_1 obtained with TDH (a), TRS (b) and RT-NAH (c). Backpropagation of a 1000 Hz impulse from 10 cm to 1 cm for A_2. The red circle represents the source position and size.

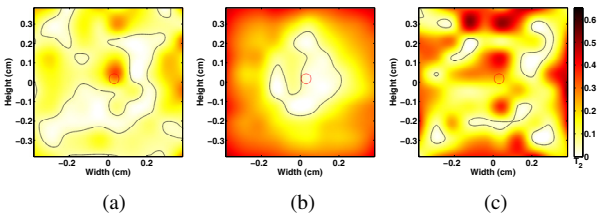

Figure 5: Spatial maps for indicator T_2 obtained with TDH (a), TRS (b) and RT-NAH (c). Backpropagation of a 1000 Hz impulse from 10 cm to 1 cm for A_2. The red circle represents the source position and size.

Examples of mapping results for T_1 and T_2 are given in Figure 4 and Figure 5 for the three methods. The radiating source is the loudspeaker A_2 driven by a 1000 Hz impulse signal and the signal is back-propagated from 10 cm to 1 cm. As shown on Figure 4, TDH seems to be the more effective method for T_1 indicator for the studied back-propagation distance (10 cm). TRS method provides high level of T_1 close to the source location while RT-NAH method gives high levels of T_1 in a small area near the source and in an extended area farther the source but also shows low levels of T_1 at the edges of the studied area. Figure 5 shows that for the studied backpropagation distance, TDH and TRS methods present the best results. Spatial distributions for each methods are different: TRS estimates correctly the pressure level close to the source location while TDH presents good results in a more spreaded way. For the two indicators T_1 and T_2, edge effects can be noticed for RT-NAH and TRS results.

Figure 6 shows E_n obtained for the three methods with radiating source A_2 driven by a 1000 Hz impulse signal, back-propagated from 10 cm to 1 cm. TDH and RT-NAH errors present peaks of magnitude at times corresponding to high levels of magnitude for the BP pressure field (see Fig. 2). Reconstruction errors $E_n(t)$ obtained with TRS method is less oscillating in time and appears to have lower values.

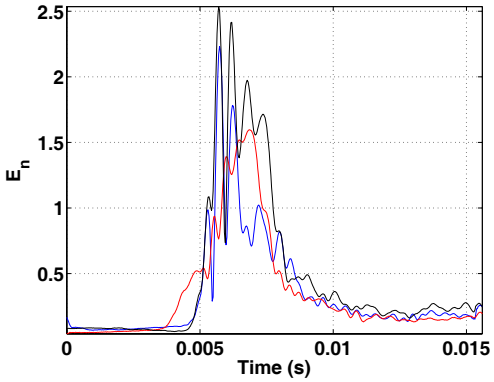

Figure 6: Spatial error $E_n(t)$ obtained with the three methods for a 9 cm back-propagation distance (1000 Hz impulse emitted by A_2) - Blue: TDH - Red: TRS - Black: RT-NAH.

In the following, for the sake of compactness of this paper, T_1 and T_2 maps and time domain evolution of E_n will not be presented for each studied back-propagation. In order to compare imaging efficiency for the three methods in a synthetic way, we rather present the mean, median, and standard deviation values of each indicators for each experiment.

4.3 Influence of back-propagation distance

In all experiment presented in this subsection, the loudspeakers are driven by a 1000 Hz impulse signal. T_1 evolution with back-propagation distance is given in Figure 7(a) for a centered source A_2 and in Figure 7(b) for an off-centered source A_5. For a distance of 5 cm, TDH and TRS methods appear to be really effective for both sources. For distances of 10 and 15 cm, TDH gives the best mean values while the median value of RT-NAH gives better results for the centered source and a distance of 15 cm. For distances of 20 and 25 cm, results obtained using TDH method are more deteriorating than with the two other methods, especially for the centered source. RT-NAH method gives the best results for T_1 at large back-propagation distances (20/25 cm).

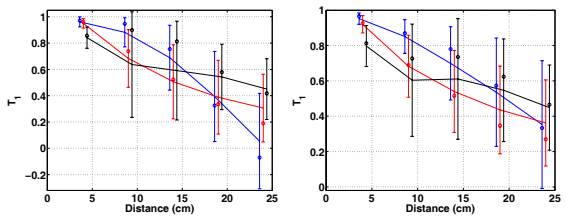

(a) (b)

Figure 7: Variation of T_1 against back-propagation distance for the 1000 Hz impulse signal; (a) source A_2, (b) source A_5 - Blue: TDH - Red: TRS - Black: RT-NAH.

T_2 evolution with back-propagation distance is given in Figure 8 for the same loudspeakers as in Fig. 7. Similarly to T_1 indicator results, both methods TDH and TRS are more effective than RT-NAH for a distance of 5 cm. For the centered source and a back-propagation distance of 10 cm, TDH gives better results than the two others. For backpropagation distances larger than 15 cm, TDH and RT-NAH results are deteriorating while TRS method gives good results especially for 25 cm and a centered source. RT-NAH results show a less accurate reconstruction than the two other methods for a centered source. For the off-centered source, TDH and RT-NAH give good results for all distances while TRS results are deteriorating with an increase of the distance.

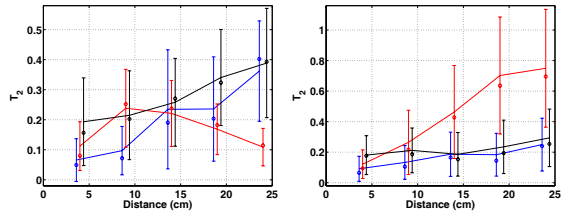

(a) (b)

Figure 8: Variation of T_2 against back-propagation distance for the 1000 Hz impulse signal; (a) source A_2, (b) source A_5 - Blue: TDH - Red: TRS - Black: RT-NAH.

E_n evolution with back-propagation distance is shown in Figure 9 for the source A_2 (a) and the source A_5 (b). Figure 9(a) shows that for the centered source and whatever the distance, TRS method gives best results for mean values than TDH and RT-NAH. The three methods present an increase of errors with the distance.

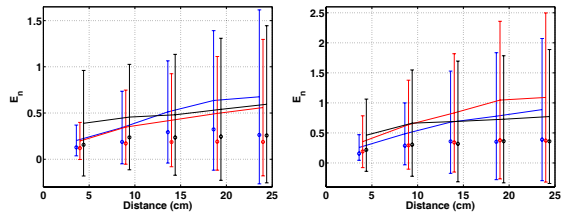

(a) (b)

Figure 9: Variation of E_n against back-propagation distance for the 1000 Hz impulse signal; (a) source A_2, (b) source A_5 - Blue: TDH - Red: TRS - Black: RT-NAH.

Figure 9(b) shows that for the off-centered source, TDH method provides the smallest mean error for small distances (5/10 cm) and RT-NAH method provides the smallest mean error for large distances (20/25 cm). On the other hand, median values are really close for the three methods and remain constant with the distance, except at a 5 cm back-propagation distance, exhibiting smaller median values.

4.4 Influence of frequency content

In this subsection, we only present results obtained for two back-propagation distances of 5 cm and 20 cm. Loudspeakers are driven by impulse signals with different central frequencies. Since the signal spectra correspond to Hanning windows between 0 and $2f_c$, it should be noted that the spatial Shannon theorem is not fulfilled for central frequencies above 1335 Hz. Results for these frequencies allow to investigate the ability of the methods to back-propagate high frequencies with an under-sampled array.

The evolution of indicator T_1 as a function of signal's central frequency is given in Figure 10 for sources A_2 and A_5. For a back-propagation distance of 5 cm and for frequencies below 1335 Hz, TDH and TRS methods are similarly effective for both sources while RT-NAH shows more difficulties to reproduce the phase difference. For frequencies above 1335 Hz, the three methods provide similar results and degrade in a similar way when the Shannon sampling theorem is not fulfilled. For a back-propagation distance of 20 cm, the same evolutions are observed for the two sources: for low frequencies ($\leq$ 750 Hz) TDH gives the best results but its T_1 values decrease with frequency. On the other hand, RT-NAH method is the best for 1000 Hz while TRS method seems to be more robust at high frequency, when the spatial sampling theorem is not fulfilled.

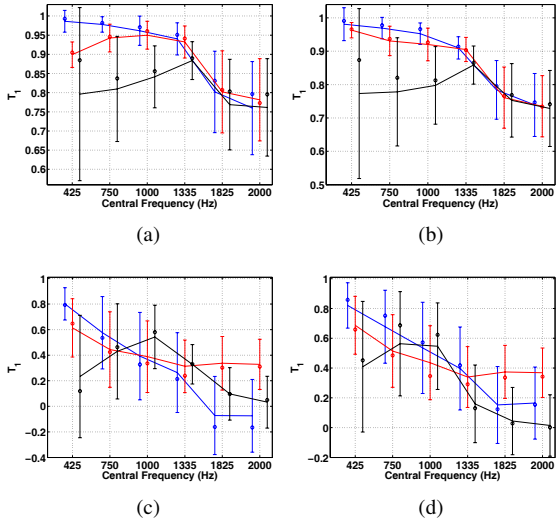

(a) (b)

(c) (d)

Figure 10: Variation of T_1 against central frequency of the impulse signals; (a) source A_2 at 5 cm, (b) source A_5 at 5 cm (c) source A_2 at 20 cm, (d) source A_5 at 20 cm - Blue: TDH - Red: TRS - Black: RT-NAH.

The evolution of indicator T_2 as a function of signal's central frequency is given in Figure 11 for the source A_2 and the source A_5. For this indicator, TDH seems to be the most reliable method to describe correctly signal amplitudes for a distance of 5 cm, even if RT-NAH gives similar results for frequencies above 1335 Hz. On the contrary, TRS method presents better results than RT-NAH for frequencies below 1335 Hz and shows the best results for low frequencies when the off-centered source is imaged. For a 20 cm back-propagation distance, different trends are observed: for a centered source, except for the low frequency limit, the best results are obtained using TRS method. Stable correct values

are obtained using TDH method and it seems that RT-NAH method has difficulties to reconstruct the true amplitudes, particularly above 1000 Hz. For an off-centered source, TRS method and to a lesser extent RT-NAH method are deteriorating with an increase of frequency while TDH method remains constant. Up to 1335 Hz, THD and RT-NAH methods give similar T2 values.

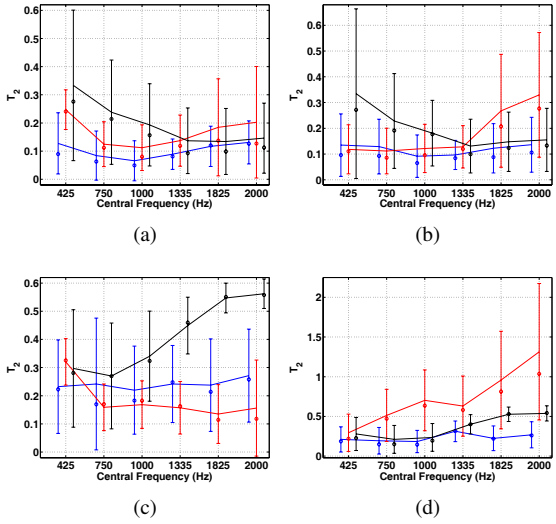

Figure 11: Variation of T_2 against central frequency of the impulse signals; (a) source A_2 at 5 cm, (b) source A_5 at 5 cm (c) source A_2 at 20 cm, (d) source A_5 at 20 cm - Blue: TDH - Red: TRS - Black: RT-NAH.

The evolution of the error criterion E_n with the central frequency of the impulse signal is given in Figure 12 for sources A_2 and A_5. For a 5 cm back-propagation distance, TDH and TRS give very small errors while RT-NAH provides larger errors for central frequencies below 1335 Hz. Results are similar for higher frequencies. For a 20 cm BP distance, results are similar for the three methods, even if RT-NAH and TRS seem better when the frequency increases for a centered source and RT-NAH and TDH remain constant for an off-centered source.

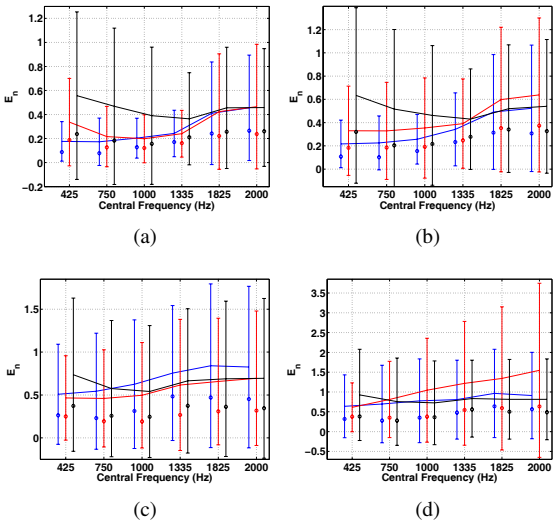

Figure 12: Variation of E_n against central frequency of the impulse signals; (a) source A_2 at 5 cm, (b) source A_5 at 5 cm (c) source A_2 at 20 cm, (d) source A_5 at 20 cm - Blue: TDH - Red: TRS - Black: RT-NAH.

5 Conclusion

Results obtained for the three studied imaging techniques in the case of point-like sources show that the different methods are complementary. Depending on the back-propagation distance or the frequency range of the tested source, a particular method should be chosen. This preliminary report is the first step of an ongoing project. In near future, complementary experiments will be conducted, such as multiple simultaneously driven loudspeakers or impacted plates. Eventually, industrial cases will also be investigated. A special attention will be dedicated to the resolution ability of the different methods. Note that, other formulations of the three methods used here should also be included:

- For RT-NAH, as the method implemented in the present paper is based on inverse Wiener filtering, no regularization was involved and it is possible that using the method proposed in [5] would improve the results.
- For TDH, the direct and inverse spatial Fourier transform can be suppressed when using a propagator written in the (x, y, ω) domain. This formulation involves a spatial convolution and has been shown to be more suited to large distance propagation [2] though slightly increasing the computation time.
- For TRS, the implementation used in the present study makes use of an approximated extrapolation of the pressure field normal derivatives thanks to the sink method. Even if the present study shows satisfying results, more accurate reconstructions could be achieved using a double layer measurement array.

References

[1] J. Hald, "Time Domain Acoustical Holography and its applications", Sound and Vibration, 16-24, (February 2001)

[2] O. de La Rochefoucauld, "Resolution of the space/time inverse problem in near field acoustical holography: Application to the radiation of non stationary industrial sources," Ph.D. dissertation (in french), Université du Maine, Le Mans, France (2002)

[3] V. Grulier, S. Paillasseur, J.-H. Thomas, J.-C. Pascal, J.-C. Le Roux, "Forward propagation of time evolving acoustic pressure: Formulation and investigation of the impulse response in time-wavenumber domain", *J. Acoust. Soc. Am* **126**(5), 2367-2378 (2009)

[4] J.-H. Thomas, V. Grulier, S. Paillasseur, J.-C. Pascal, J.-C. Le Roux, "Real-time near-field acoustic holography for continuously visualizing nonstationary acoustic fields", *J. Acoust. Soc. Am* **128**(6), 3554-3567 (2010)

[5] S. Paillasseur, J.-H. Thomas, J.-C. Pascal, "Regularization for improving the deconvolution in real-time near-field acoustic holography", *J. Acoust. Soc. Am* **129**(6), 3777-3787 (2011)

[6] M. Fink, D. Cassereau, A. Derode, C. Prada, P. Roux, M. Tanter, J-L. Thomas, F. Wu, "Time reversed acoustics", *Rep. Prog. Phys.* **63**, 1933-1995 (2000)

[7] J. de Rosny and M. Fink, "Overcoming the Diffraction Limit in Wave Physics Using a Time-Reversal Mirror and a Novel Acoustic Sink", Phys. Rev. Lett. **89**, 124301-1–124301-4 (2002).

[8] E. Bavu, A. Berry, "Super-resolution imaging of sound sources in free field using a numerical time-reversal sink", *Acta Acust. United Ac.*, **95** (4), 595-606 (2009)